Pergamon

0045-7949(94)E0090-O

Computers & Structures Vol. 53, No. 3, pp. 739–754, 1994
Elsevier Science Ltd
Printed in Great Britain
0045-7949/94 $7.00 + 0.00

LOCAL AND MODELS FOR NONLINEAR DYNAMIC ANALYSIS OF MULTI-STORY SHEAR BUILDINGS SUBJECT TO EARTHQUAKE LOADING

S. Rahman† and **M. Grigoriu**‡

†Department of Engineering Mechanics, 505 King Avenue, Battelle, Columbus, OH 43201, U.S.A.
‡Department of Structural Engineering, Cornell University, Ithaca, NY 14853, U.S.A.

(*Received* 21 *September* 1992)

Abstract—This paper proposes a global hysteretic model and establishes analytical relationship between the parameters of local and global hysteretic models for seismic analysis of multi-story shear type buildings. In both models, the analysis involves hysteretic constitutive laws commonly used in earthquake engineering to represent restoring forces and nonlinear dynamic analysis to estimate the seismic response of structural systems. However, when the global model is used, the dimension of dynamic structural analysis becomes much smaller, and hence, the computational effort can be reduced significantly. From the proposed relationship between these models, the local hysteretic behavior and damage can be recovered from analysis based on global models. Several numerical examples based on nondegrading and degrading hysteresis of both single- and multi-degree-of-freedom shear beam systems are presented to illustrate and validate the proposed methodology. The results suggest that the global model can provide accurate estimates of seismic response and damage characteristics of structural systems.

1. INTRODUCTION

The conventional seismic analysis of discrete, nonlinear structural systems is based on a concentrated plasticity model, which describes the local restoring force characteristics at the critical components of interest. For building frames, these restoring force–deformation relationships are defined locally at the member level for shear type buildings (e.g., column shear force versus relative column end displacement) or at the cross-section level for general yielding frames (e.g., bending moment versus curvature or rotation at the end joints of a beam–column). Given a hysteretic model, the parameters of such local restoring forces are usually estimated by experimental calibration. Using this local model with the restoring forces adequately defined at all critical components, the equations of motion can be directly integrated to yield various structural response characteristics. However, the inconvenience with regard to the applicability of a local model as a practical analysis tool for large structural systems is not of a minor nature. This is obviously because of the large dimension in which the stress analysis has to be performed. The computational effort is still significant and time-consuming even with the recent development of numerical techniques and computational facilities. These issues become more significant when numerous deterministic analyses are required in a full probabilistic analysis. It is thus desirable to perform structural dynamic analysis on some reduced dimension to lessen the computational burden without any serious loss of accuracy in the results. In principle, this can be achieved by using a global model, which describes the restoring force–deformation characteristics at a global level (e.g., story shear force versus relative story displacements for shear type buildings). But, when such a model is to be used, it is required to know *a priori* the parameters which govern the global hysteretic characteristics of structural systems. Currently, there are no rational methodologies available for determining these global parameters.

In addition, some of the parameters of the local restoring forces are usually related to known physical properties, such as the strength and/or stiffness of structural components. Any change in the values of these time-variant parameters due to a potential seismic event is thus indicative of induced damage due to possible structural degradation. This suggests that conceptual models of *local damage indices* can be developed from the known state of local parameters. During a seismic event, such local indices not only describe the progression of structural damage for seismic performance evaluation, but also provide a unique characterization of the structural state due to one-to-one correspondence with the parameters of the local restoring forces. Traditionally, however, seismic damage tolerance is evaluated by *global damage indices* which are obtained from heuristic combinations of local damage measures. Numerous forms of such global indices are reported in the current literature of earthquake engineering [1, 2]. Most of them are defined quite arbitrarily without accounting for the mechanistic relations between local and global damage measures. Thus, the current measure of global damage (i) can not characterize the structural state uniquely, (ii) provides only a crude estimate of structural performance during seismic events, and (iii) can not be used to assess structural vulnerability to future loadings [3, 4].

This paper develops a global hysteretic model and establishes an analytic relationship between the parameters of the local and global hysteretic models for the seismic analysis of multi-story shear buildings. The method of analysis is based on (i) a state-of-the-art endochronic model [3, 5–9] for restoring forces and (ii) nonlinear dynamic analysis for estimating the structural response to earthquakes. Both nondegrading and degrading systems are considered. Several numerical examples on single- and multi-degree-of-freedom systems are presented to illustrate and validate the proposed methodology.

2. SHEAR BEAM MODELS

Consider the shear beam model of n-degree-of-freedom systems shown in Fig. 1(a). The second order differential equation representing the equation of motion of the kth mass (floor) exhibited in Fig. 1(b) is given by ($k = 1$ for the first floor and $k = n$ for the top floor)

$$\sum_{j=1}^{k} \ddot{U}_j(t) + W(t) + \frac{g_k}{m_k} - (1-\delta_{kn})\frac{g_{k+1}}{m_k} = 0, \quad (1)$$

where $U_k(t)$ is the displacement of the kth mass with respect to displacement of the $(k-1)$th mass (except when $k = 1$), m_k is the kth mass, g_k is the kth general restoring force, $W(t)$ is the external dynamic excitation representing ground acceleration due to earthquakes, n is the total number of masses (floors), and δ_{kn} is the Kronecker delta, i.e., $\delta_{kn} = 1$ for $k = n$ or zero otherwise. When the $(k-1)$th equation is subtracted from the kth equation (except when $k = 1$), the resulting decoupled equation takes the form

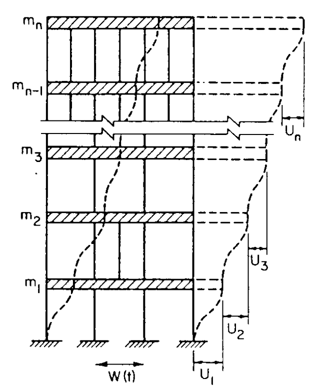

(a) Shear Beam Idealization

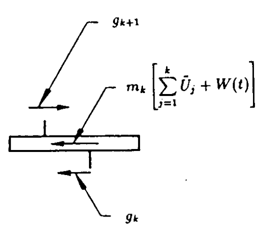

(b) Forces Acting on kth Mass

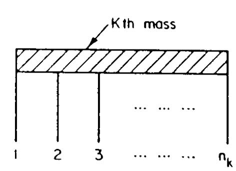

(c) Columns at kth Story

Fig. 1. Shear beam idealization of framed structures.

$$\ddot{U}_k(t) - (1-\delta_{k1})\frac{g_{k-1}}{m_{k-1}} + \left[1 + (1-\delta_{k1})\frac{m_k}{m_{k-1}}\right]\frac{g_k}{m_k} - (1-\delta_{kn})\frac{m_{k+1}}{m_k}\frac{g_{k+1}}{m_{k+1}} = -\delta_{k1}W(t) \quad (2)$$

with the initial conditions $U_k(0) = 0$ and $\dot{U}_k(0) = 0$ in which once again δ_{k1}, δ_{kn} are Kronecker deltas introduced for the equation to be valid when $k = 1$ and $k = n$.

3. LOCAL RESTORING FORCE

Suppose that the kth story of a building consists of n_k individual columns (Fig. 1c) each of which may be associated with widely different stiffness and strength characteristics. The total restoring force g_k at the kth story can be obtained from

$$g_k = c_k\dot{U}_k(t) + \sum_{l=1}^{n_k}\alpha_{kl}k_{kl}U_k(t) + \sum_{l=1}^{n_k}(1-\alpha_{kl})k_{kl}Z_{kl}(t) \quad (3)$$

in which c_k is the kth constant damping (viscous) coefficient, α_{kl} is the parameter defining the participation of the linear restoring force, k_{kl} is the stiffness, and $Z_{kl}(t)$ is the hysteretic (auxiliary) variable, all of which are associated with the lth column of the kth story. It is assumed here that the evolution of $Z_{kl}(t)$ can be modeled by a first-order nonlinear ordinary differential equation [6–9]

$$\dot{Z}_{kl}(t) = A_{kl}(t)\dot{U}_k(t) - \beta_{kl}|\dot{U}_k(t)| \times |Z_{kl}(t)|^{\mu_k - 1}Z_{kl}(t) - \gamma_{kl}\dot{U}_k(t)|Z_{kl}(t)|^{\mu_k}, \quad (4)$$

where β_{kl}, γ_{kl} and μ_k are the time-invariant parameters and $A_{kl}(t)$ is the time-varying parameter of the local hysteretic restoring force model. The parameter $A_{kl}(t)$ which controls column stiffness and strength degradation is assumed to follow an energy-based deterioration rule given by [10]

$$A_{kl}(t) = A_{kl}(0) - \delta_{A_{kl}}\int(1-\alpha_{kl})k_{kl}Z_{kl}\,\mathrm{d}U_k(t) \quad (5)$$

in which $\delta_{A_{kl}}$ is a constant rate of local deterioration. Note that the degradation law in eqn (5) is defined here quite arbitrarily. It is obtained from one of the many choices available in the current literature. Further study with more realistic buildings needs to be undertaken to make decisions regarding the proper selection of deterioration laws. Following the state vector approach with the designation of state variables $\theta_{k1}(t) = U_k(t)$, $\theta_{k2}(t) = \dot{U}_k(t)$, and $\theta_{k3}(t) = Z_{k1}(t), \ldots, \theta_{k,2+n_k}(t) = Z_{k,n_k}(t)$ at the kth story, the equivalent system of first order differential equations corresponding to eqns (2) and (4) becomes

$$\begin{aligned}
\dot{\theta}_{k1}(t) &= \theta_{k2}(t)\\
\dot{\theta}_{k2}(t) &= (1-\delta_{k1})\frac{g_{k-1}}{m_{k-1}} - \left[1 + (1-\delta_{k1})\frac{m_k}{m_{k-1}}\right]\frac{g_k}{m_k} + (1-\delta_{kn})\frac{m_{k+1}}{m_k}\frac{g_{k+1}}{m_{k+1}} - \delta_{k1}W(t)\\
\dot{\theta}_{k3}(t) &= A_{k1}(t)\theta_{k2}(t) - \beta_{k1}|\theta_{k2}(t)||\theta_{k3}(t)|^{\mu_k - 1}\theta_{k3}(t) - \gamma_{k1}\theta_{k2}(t)|\theta_{k3}(t)|^{\mu_k}\\
&\vdots\\
\dot{\theta}_{k,2+n_k}(t) &= A_{k,n_k}(t)\theta_{k2}(t) - \beta_{k,n_k}|\theta_{k2}(t)||\theta_{k,2+n_k}(t)|^{\mu_k - 1}\theta_{k,2+n_k}(t) - \gamma_{k,n_k}\theta_{k2}(t)|\theta_{k,2+n_k}(t)|^{\mu_k}
\end{aligned} \quad (6)$$

which can be recast in a compact form

$$\dot{\boldsymbol{\theta}}(t) = \mathbf{h}(\boldsymbol{\theta}(t), t; \mathbf{A}(t)) \quad (7)$$

with the initial conditions $\boldsymbol{\theta}(0) = \mathbf{0}$, where $\boldsymbol{\theta}(t) = \{\ldots, \theta_{k1}(t), \theta_{k2}(t), \theta_{k3}(t), \ldots, \theta_{k,2+n_k}(t), \ldots\}^{\mathrm{T}}$ is a real $(2n + \Sigma_{k=1}^{n} n_k)$-dimensional response state vector, $\mathbf{A}(t) = \{\ldots, A_{k1}(t), A_{k2}(t), \ldots, A_{k,n_k}(t), \ldots\}^{\mathrm{T}}$ is a real $(\Sigma_{k=1}^{n} n_k)$-dimensional damage state vector representing the state of the time-variant parameters in the local restoring force, $\mathbf{h}(\cdot)$ is a vector function, $\mathbf{0}$ is a null vector, and the superscript T is a symbol for the transpose of a general vector. At any time t during a potentially damaging seismic event, $\mathbf{A}(t)$ characterizes uniquely the state of structural damage due to any stiffness degradation or strength deterioration.

4. GLOBAL RESTORING FORCE

Suppose that the total restoring force g_k at the kth story can also be modeled globally as

$$g_k = c_k\dot{U}_k(t) + \alpha_k^* k_k^* U_k(t) + (1-\alpha_k^*)k_k^* Z_k^*(t) \quad (8)$$

in which α_k^* is the global parameter defining the participation of the kth linear restoring force, k_k^* is the kth story stiffness, and $Z_k^*(t)$ is the single kth global hysteretic variable, the evolution of which can be modeled by a similar first-order nonlinear ordinary differential equation

$$\dot{Z}_k^*(t) = A_k^*(t)\dot{U}_k(t) - \beta_k^*|\dot{U}_k(t)||Z_k^*(t)|^{\mu_k^* - 1}Z_k^*(t) - \gamma_k^*\dot{U}_k(t)|Z_k^*(t)|^{\mu_k^*}, \quad (9)$$

where $\beta_k^*, \gamma_k^*, \mu_k^*$ are the time-invariant parameters and $A_k^*(t)$ is the time-varying parameter of the global hysteretic restoring force model. The parameter $A_k^*(t)$ which now controls story stiffness and strength degradation is expected to follow a similar degradation rule

$$A_k^*(t) = A_k^*(0) - \delta_{A_k}^* \int (1-\alpha_k^*) k_k^* Z_k^*(t)\, \mathrm{d}U_k(t) \quad (10)$$

in which $\delta_{A_k}^*$ represents a constant rate of global deterioration. Following the designation of state variables $\theta_{k1}^*(t) = U_k(t)$, $\theta_{k2}^*(t) = \dot{U}_k(t)$ and $\theta_{k3}^*(t) = Z_k^*(t)$, the equivalent system of first order differential equations corresponding to eqns (2) and (9) becomes

$$\dot{\theta}_{k1}^*(t) = \theta_{k2}^*(t)$$

$$\dot{\theta}_{k2}^*(t) = (1-\delta_{k1})\frac{g_{k-1}}{m_{k-1}} - \left[1 + (1-\delta_{k1})\frac{m_k}{m_{k-1}}\right]\frac{g_k}{m_k} + (1-\delta_{kn})\frac{m_{k+1}}{m_k}\frac{g_{k+1}}{m_{k+1}} - \delta_{k1} W(t)$$

$$\dot{\theta}_{k3}^*(t) = A_k^*(t)\theta_{k2}^*(t) - \beta_k^* |\theta_{k2}^*(t)| |\theta_{k3}^*(t)|^{\mu_k^*-1}\theta_{k3}^*(t) - \gamma_k^* \theta_{k2}^*(t) |\theta_{k3}^*(t)|^{\mu_k^*}, \quad (11)$$

which can be recast in a compact form

$$\dot{\boldsymbol{\theta}}^*(t) = \mathbf{h}^*(\boldsymbol{\theta}^*(t), t; \mathbf{A}^*(t)) \quad (12)$$

with the initial conditions $\boldsymbol{\theta}^*(0) = \mathbf{0}$, where $\boldsymbol{\theta}^*(t) = \{\ldots, \theta_{k1}^*(t), \theta_{k2}^*(t), \theta_{k3}^*(t), \ldots\}^{\mathrm{T}}$ is the $3n$-dimensional response state vector, $\mathbf{A}^*(t) = \{A_1^*(t), A_2^*(t), \ldots, A_n^*(t)\}^{\mathrm{T}}$ is the n-dimensional damage state vector representing the state of time-variant parameters in the global restoring force, and $\mathbf{h}^*(\cdot)$ is a vector function. Note that in both local and global models, the dynamic structural analysis can be viewed as a nonlinear initial-value problem with the system of the differential equations described above. But, the dimension of $\boldsymbol{\theta}^*(t)$ is much smaller than that of $\boldsymbol{\theta}(t)$, particularly when the total number of columns n_k for all the stories $k = 1, 2, \ldots, n$ is very large. Hence, when the global model is used, the computational effort in solving the initial value problem can be reduced significantly. Application of the global model, however, will require estimation of its parameters from the known calibrated parameters of the local model. They are discussed in the forthcoming section.

5. RELATIONSHIP BETWEEN LOCAL AND GLOBAL PARAMETERS

Consider the kth total restoring force g_k in eqn (3) obtained from the local restoring forces. Following simple algebra, it can be shown that

$$g_k = c_k \dot{U}_k(t) + \sum_{l=1}^{n_k} w_{kl}\alpha_{kl} \sum_{l=1}^{n_k} k_{kl} U_k(t) + \left[1 - \sum_{l=1}^{n_k} w_{kl}\alpha_{kl} \times \frac{\sum_{l=1}^{n_k} w_{kl}\alpha_{kl} Z_{kl}(t)}{\sum_{l=1}^{n_k} w_{kl} Z_{kl}(t) \sum_{l=1}^{n_k} w_{kl}\alpha_{kl}}\right] \times \sum_{l=1}^{n_k} k_{kl} \sum_{l=1}^{n_k} w_{kl} Z_{kl}(t) \quad (13)$$

in which

$$w_{kl} = \frac{k_{kl}}{\sum_{l=1}^{n_k} k_{kl}} \quad (14)$$

is the stiffness-based weighting coefficient. Further simplification of above equation can be accomplished by noting that

$$\frac{\sum_{l=1}^{n_k} w_{kl}\alpha_{kl} Z_{kl}(t)}{\sum_{l=1}^{n_k} w_{kl} Z_{kl}(t) \sum_{l=1}^{n_k} w_{kl}\alpha_{kl}} \to 1 \quad (15)$$

when $\alpha_{kl} \to 0$ *or* α_{kl} does not vary within the columns at a given story. In earthquake engineering, this is not a significant limitation as the quantity α_{kl}, which also represents the ratio of post- to pre-yield stiffnesses, is indeed small for realistic material models. Recent calibration with the laboratory data reported in [11] suggests that $\alpha_{kl} = 0.04$ for steel and $\alpha_{kl} = 0.02$ for reinforced concrete. Thus, with this approximation, eqn (13) takes the form

$$g_k = c_k \dot{U}_k(t) + \sum_{l=1}^{n_k} w_{kl}\alpha_{kl} \sum_{l=1}^{n_k} k_{kl} U_k(t) + \left(1 - \sum_{l=1}^{n_k} w_{kl}\alpha_{kl}\right) \sum_{l=1}^{n_k} k_{kl} \sum_{l=1}^{n_k} w_{kl} Z_{kl}(t) \quad (16)$$

which when compared with the kth total restoring force g_k in eqn (8) obtained from the global restoring force gives

$$\alpha_k^* = \sum_{l=1}^{n_k} w_{kl}\alpha_{kl}, \quad k_k^* = \sum_{l=1}^{n_k} k_{kl}$$

and

$$Z_k^*(t) = \sum_{l=1}^{n_k} w_{kl} Z_{kl}(t). \tag{17}$$

5.1. *Time-invariant parameters*

Consider the rate equation of the global hysteretic variable $Z_k^*(t)$ in eqn (17) which can be expanded as follows:

$$\begin{aligned}\dot{Z}_k^*(t) &= \sum_{l=1}^{n_k} w_{kl}\dot{Z}_{kl}(t)\\ &= \sum_{l=1}^{n_k} w_{kl}[A_{kl}(t)\dot{U}_k(t) - \beta_{kl}|\dot{U}_k(t)||Z_{kl}(t)|^{\mu_k-1}Z_{kl}(t) - \gamma_{kl}\dot{U}_k(t)|Z_{kl}(t)|^{\mu_k}]\\ &= \sum_{l=1}^{n_k} w_{kl}A_{kl}(t)\dot{U}_k(t) - \frac{\sum_{l=1}^{n_k} w_{kl}\beta_{kl}|Z_{kl}(t)|^{\mu_k-1}Z_{kl}(t)}{\left|\sum_{l=1}^{n_k} w_{kl}Z_{kl}(t)\right|^{\mu_k-1}\sum_{l=1}^{n_k} w_{kl}Z_{kl}(t)}|\dot{U}_k(t)|\left|\sum_{l=1}^{n_k} w_{kl}Z_{kl}(t)\right|^{\mu_k-1}\\ &\quad\times\sum_{l=1}^{n_k} w_{kl}Z_{kl}(t) - \frac{\sum_{l=1}^{n_k} w_{kl}\gamma_{kl}|Z_{kl}(t)|^{\mu_k}}{\left|\sum_{l=1}^{n_k} w_{kl}Z_{kl}(t)\right|^{\mu_k}}\dot{U}_k(t)\left|\sum_{l=1}^{n_k} w_{kl}Z_{kl}(t)\right|^{\mu_k}.\end{aligned} \tag{18}$$

Comparison of the above equation with eqn (9) suggests

$$\mu_k^* = \mu_k, \quad A_k^*(t) = \sum_{l=1}^{n_k} w_{kl}A_{kl}(t) \tag{19}$$

and

$$\beta_k^* = \frac{\sum_{l=1}^{n_k} w_{kl}\beta_{kl}|Z_{kl}(t)|^{\mu_k-1}Z_{kl}(t)}{\left|\sum_{l=1}^{n_k} w_{kl}Z_{kl}(t)\right|^{\mu_k-1}\sum_{l=1}^{n_k} w_{kl}Z_{kl}(t)},$$

$$\gamma_k^* = \frac{\sum_{l=1}^{n_k} w_{kl}\gamma_{kl}|Z_{kl}(t)|^{\mu_k}}{\left|\sum_{l=1}^{n_k} w_{kl}Z_{kl}(t)\right|^{\mu_k}}. \tag{20}$$

Note that the expressions for the global parameters in eqn (20) involve local hysteretic variables $Z_{kl}(t)$ in both numerator and denominator which in turn may be dependent on external load parameters. This has the immediate effect that the global parameters β_k^* and γ_k^* are no longer time-invariant as their counterparts are at the local level. Thus, when a global modeling is adopted, the exact determination of these parameters is not possible due to lack of *a priori* knowledge regarding the evolution of local hysteretic variables.

For an earthquake type of loading, it is however, feasible to search for the approximate evaluation of the above global parameters and still treat them as time-invariant hysteretic parameters. Two extreme cases based on the magnitude of the seismic intensity can be perceived. When the intensity of seismic noise is not extremely large, the time span during which large differences in the values of $Z_{kl}(t)$ may occur can be neglected. This will allow approximation of $Z_{kl}(t)$ to be a common time function (say, $\hat{Z}_k(t)$) thus simplifying eqn (20) to

$$\beta_k^* \simeq \sum_{l=1}^{n_k} w_{kl}\beta_{kl} \quad \text{and} \quad \gamma_k^* \simeq \sum_{l=1}^{n_k} w_{kl}\gamma_{kl}. \tag{21}$$

On the other hand, when the intensity of seismic noise is very large, it can be argued that $Z_{kl}(t)$ assumes its maximum value $Z_{kl,\max}(0)$ most of the time during ground motion. The largest value $Z_{kl,\max}(0)$ can be easily obtained by substituting the expression for $\dot{Z}_{kl}(t)$ in eqn (4) into the following equation of maximization

$$\frac{\mathrm{d}}{\mathrm{d}U_k(t)}Z_{kl}(t) = \frac{\dot{Z}_{kl}(t)}{\dot{U}_{kl}(t)} = 0 \tag{22}$$

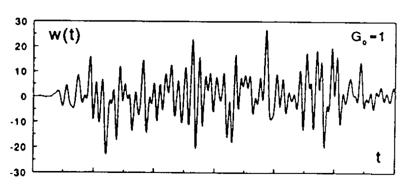

Fig. 2. A sample of modulated gaussian white noise ($G_0 = 1$).

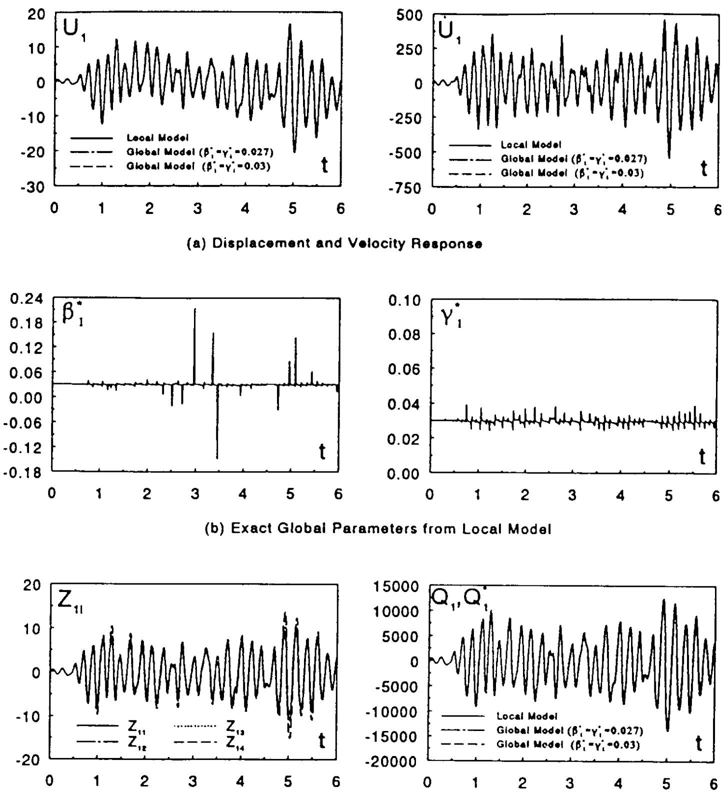

Fig. 3. Time history of various responses for nondegrading system with $G_0 = 1.0 \times 10^5$.

giving [10]

$$Z_{kl,\max}(t) = \left[\frac{A_{kl}(t)}{\beta_{kl} + \gamma_{kl}}\right]^{1/\mu_k}. \tag{23}$$

Following the replacement of $Z_{kl}(t)$ in eqn (20) by $Z_{kl,\max}(0)$ in eqn (23) at $t = 0$ along with the observation that at any time t the signs of $Z_{kl}(t)$ are the same, another estimate of the above parameters can be obtained as follows:

$$\beta_k^* \simeq \frac{\sum_{l=1}^{n_k} w_{kl}\beta_{kl}\left[\frac{A_{kl}(0)}{\beta_{kl}+\gamma_{kl}}\right]}{\left(\sum_{l=1}^{n_k} w_{kl}\left[\frac{A_{kl}(0)}{\beta_{kl}+\gamma_{kl}}\right]^{1/\mu_k}\right)^{\mu_k}}$$

and

$$\gamma_k^* \simeq \frac{\sum_{l=1}^{n_k} w_{kl}\gamma_{kl}\left[\frac{A_{kl}(0)}{\beta_{kl}+\gamma_{kl}}\right]}{\left(\sum_{l=1}^{n_k} w_{kl}\left[\frac{A_{kl}(0)}{\beta_{kl}+\gamma_{kl}}\right]^{1/\mu_k}\right)^{\mu_k}}. \tag{24}$$

The two sets of estimates of β_k^* and γ_k^* given above apply to two extreme cases of load intensity and can be used as some sort of bounds for the determination of the above parameters. When the strength of the noise is somewhat intermediate, the appropriate values of these parameters can be interpolated from these bounds.

5.2. *Time-variant parameter*

Consider the infinitesimal total hysteretic energy dissipated at the kth story from the local model [eqn (5)] which can be expanded as

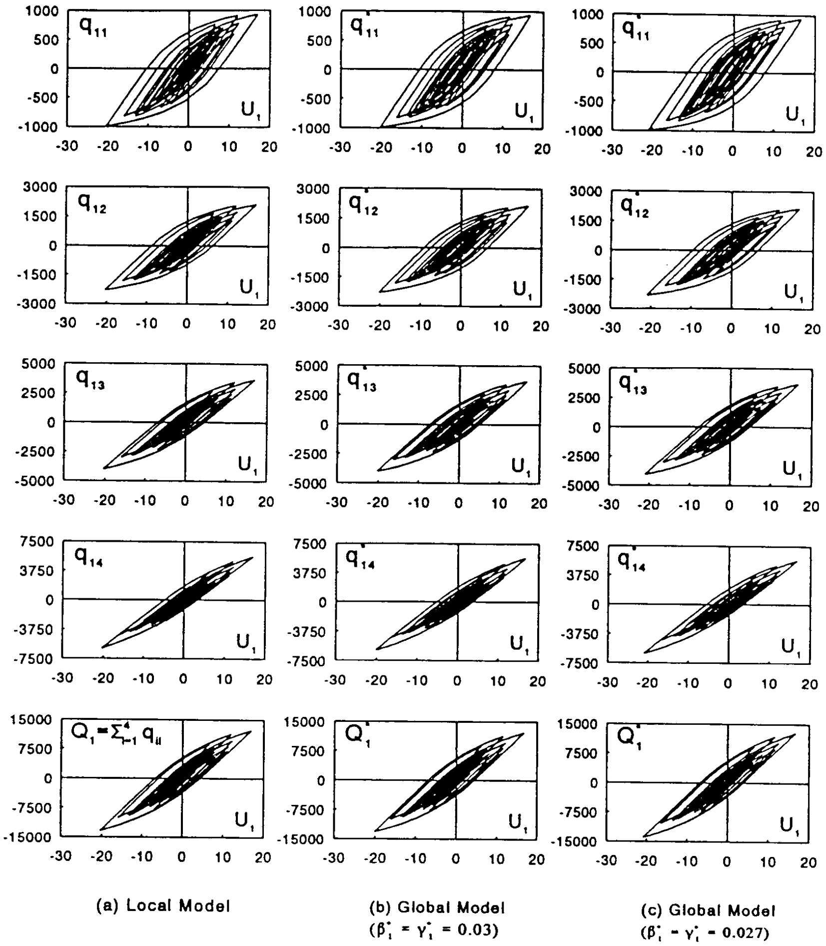

Fig. 4. Hysteretic loops for nondegrading system with $G_0 = 1.0 \times 10^5$.

$$
\begin{aligned}
&\sum_{l=1}^{n_k} (1-\alpha_{kl}) k_{kl} Z_{kl}(t)\,\mathrm{d}U_k(t) \\
&= \left[1 - \sum_{l=1}^{n_k} w_{kl}\alpha_{kl} \times \frac{\sum_{l=1}^{n_k} w_{kl}\alpha_{kl} Z_{kl}(t)}{\sum_{l=1}^{n_k} w_{kl} Z_{kl}(t) \sum_{l=1}^{n_k} w_{kl}\alpha_{kl}} \right] \\
&\quad \times \sum_{l=1}^{n_k} k_{kl} \sum_{l=1}^{n_k} w_{kl} Z_{kl}(t)\,\mathrm{d}U_k(t) \\
&= \left(1 - \sum_{l=1}^{n_k} w_{kl}\alpha_{kl} \right) \sum_{l=1}^{n_k} k_{kl} \sum_{l=1}^{n_k} w_{kl} Z_{kl}(t)\,\mathrm{d}U_k(t) \\
&= (1-\alpha_k^*) k_k^* Z_k^*(t)\,\mathrm{d}U_k(t) \qquad (25)
\end{aligned}
$$

due to similar considerations as in eqn (15). From eqn (19) with $A_{kl}(t)$ in eqn (5),

$$
\begin{aligned}
A_k^*(t) &= \sum_{l=1}^{n_k} w_{kl} \Big[A_{kl}(0) - \delta_{A_{kl}} \int (1-\alpha_{kl}) \\
&\qquad \times k_{kl} Z_{kl}(t)\,\mathrm{d}U_k(t) \Big] \\
&= A_k^*(0) - \sum_{l=1}^{n_k} w_{kl}\,\delta_{A_{kl}} \\
&\quad \times \int (1-\alpha_{kl}) k_{kl} Z_{kl}(t)\,\mathrm{d}U_k(t) \qquad (26)
\end{aligned}
$$

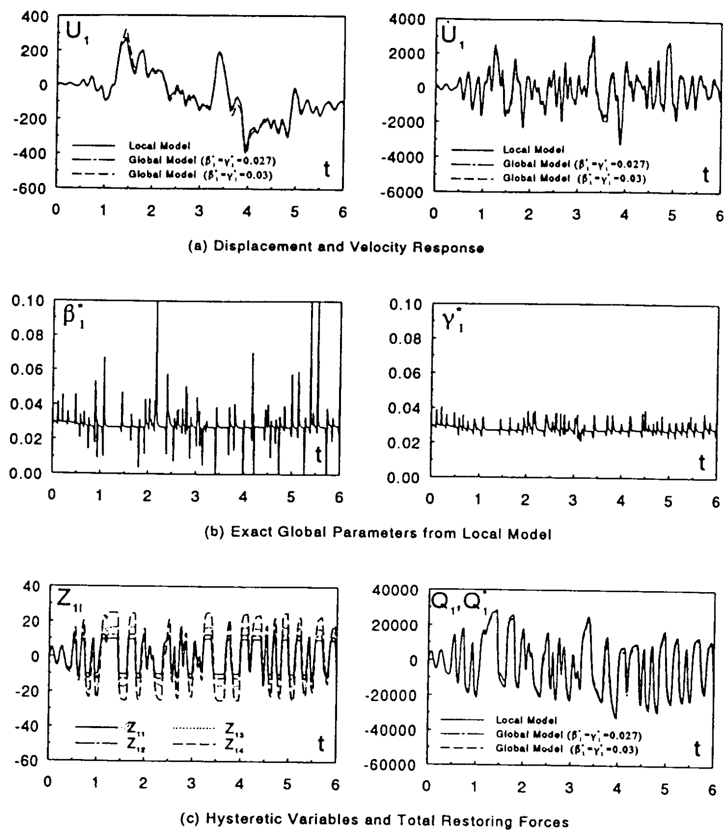

Fig. 5. Time history of various responses for nondegrading system with $G_0 = 1.0 \times 10^7$.

which can be compared with eqn (10) and the dissipated energy in eqn (25) to yield

$$\delta^*_{A_k} = \frac{\sum_{l=1}^{n_k} w_{kl}\,\delta_{A_{kl}}(1-\alpha_{kl})k_{kl}\int Z_{kl}(t)\dot{U}_k(t)\,\mathrm{d}t}{\sum_{l=1}^{n_k}(1-\alpha_{kl})k_{kl}\int Z_{kl}(t)\dot{U}_k(t)\,\mathrm{d}t} \quad (27)$$

in which the order of integral and summation operators is interchanged in the denominator, and $\mathrm{d}U_k(t) = \dot{U}_k(t)\,\mathrm{d}t$. Again, the exact evaluation of $\delta^*_{A_k}$ requires information regarding the time evolution of local hysteretic variables. Following similar considerations as in eqn (21) with small seismic intensity, the above equation reduces to

$$\delta^*_{A_k} \simeq \frac{\sum_{l=1}^{n_k} w_{kl}\,\delta_{A_{kl}}(1-\alpha_{kl})k_{kl}}{\sum_{l=1}^{n_k}(1-\alpha_{kl})k_{kl}}. \quad (28)$$

When α_{kl} is small or if it does not vary within the columns at a particular story, a more simplified form of eqn (28) results

$$\delta^*_{A_k} = \sum_{l=1}^{n_k} w_{kl}^2\,\delta_{A_{kl}}. \quad (29)$$

When the intensity of the nosie is large, similar arguments given earlier for time-invariant parameters may be applied to obtain another equation for $\delta^*_{A_k}$. However, such an estimate may not be reliable in degrading systems with large seismic intensity. This is because as time advances, $A_{kl}(t) \to 0$, and $Z_{kl,\max}(t) = [A_{kl}(t)/(\beta_{kl}+\gamma_{kl})]^{1/\mu_k} \to 0$ at a much faster rate due to the rapid loss of stiffness and/or strength. At any time during ground motion, it is difficult to anticipate the variation of $Z_{kl}(t)$ among various columns.

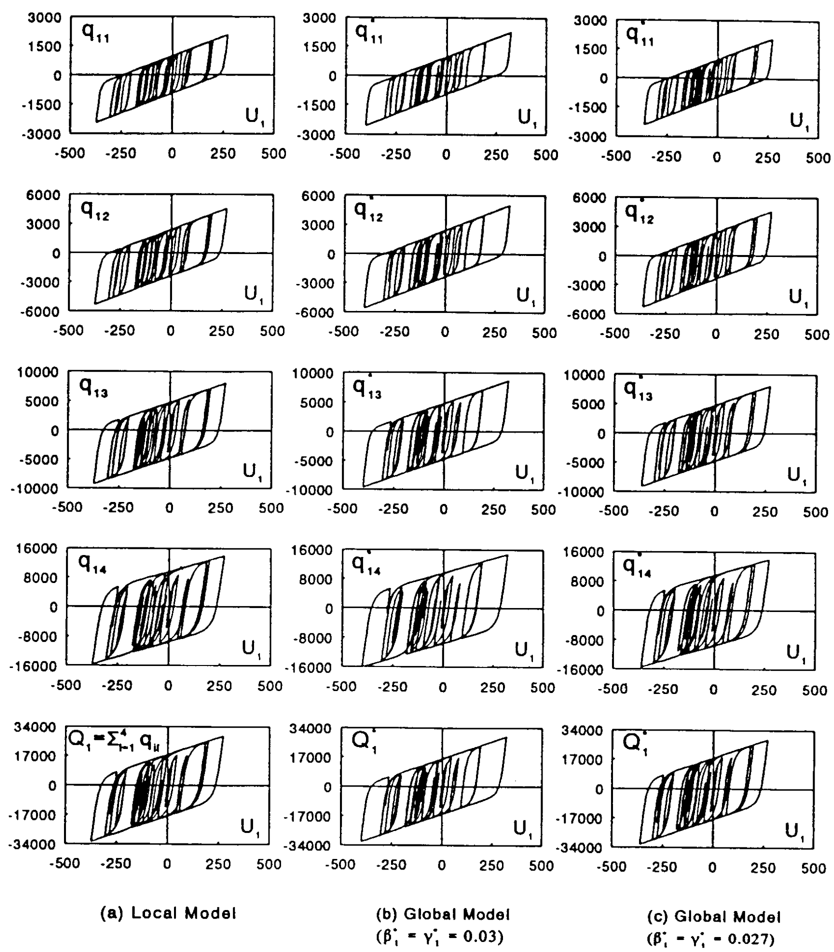

Fig. 6. Hysteretic loops for nondegrading system with $G_0 = 1.0 \times 10^7$.

6. RECOVERY OF LOCAL HYSTERESIS

Once the global parameters are estimated from the known values of local parameters, practical seismic analysis can be performed based on a global restoring force model. It is however, desirable to recover the local hysteretic behavior of structural systems. This will allow determination of local damage distribution which is uniquely related to the global model.

Consider the partitions of local and global response state vectors $\boldsymbol{\theta}(t) = \{\boldsymbol{\theta}_1(t), \boldsymbol{\theta}_2(t)\}^T$ and $\boldsymbol{\theta}^*(t) = \{\boldsymbol{\theta}^*_1(t), \boldsymbol{\theta}^*_2(t)\}^T$ in which $\boldsymbol{\theta}_1(t) = \boldsymbol{\theta}^*_1(t) = \{\ldots, U_k(t), \dot{U}_k(t), \ldots\}^T$ is the $2n$-dimensional traditional state vector (in both local and global models) comprising the relative displacement and velocity of each story mass, and $\boldsymbol{\theta}_2(t) = \{\ldots, Z_{k1}(t), \ldots, Z_{k,n_k}(t), \ldots\}^T$ and $\boldsymbol{\theta}^*_2(t) = \{\ldots, Z^*_k(t), \ldots\}^T$ are $(\Sigma^n_{k=1} n_k)$- and n-dimensional state vectors consisting of additional hysteretic variables corresponding to the local and global models, respectively. Suppose, at any time t, the state vector $\boldsymbol{\theta}^*(t)$ can be obtained by solving the global initial value problem in eqn (12). Following extraction of the component state vector $\boldsymbol{\theta}^*_1(t)$ from the global solution $\boldsymbol{\theta}^*(t)$, it can be substituted for $\boldsymbol{\theta}_1(t)$ in the local initial value problem of eqn (7) to yield a solution for the state vector $\boldsymbol{\theta}_2(t)$ of the local hysteretic variables. This way, the local hysteretic characteristics and damage of a building frame can be recovered following structural analysis based on the global model.

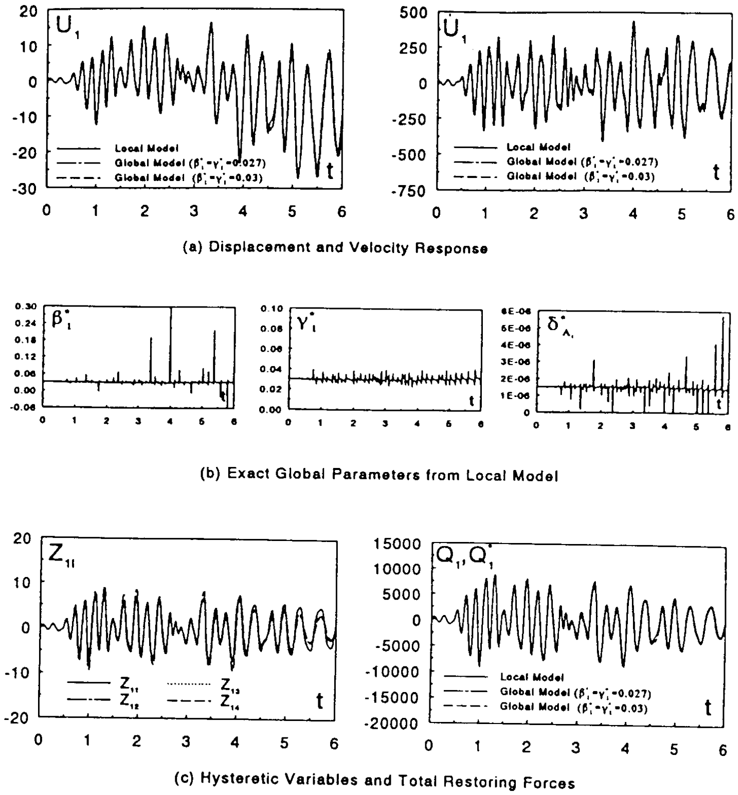

Fig. 7. Time history of various responses for degrading system with $G_0 = 1.0 \times 10^5$.

7. NUMERICAL EXAMPLES

In this section, several numerical examples are presented to illustrate and validate the proposed methodology. First, a single-degree-of-freedom system with both nondegrading and degrading restoring forces is investigated to evaluate the adequacy of the global hysteretic model in predicting various seismic response characteristics. Second, a multi-degree-of-freedom system with a more realistic design and earthquake loading is studied to compare damage measures by both local and global hysteretic models.

The nonlinear systems of first-order ordinary differential equations in the initial-value problems of both local [eqn (7)] and global [eqn (12)] models are solved by direct numerical integration. Various integrators such as the Runge–Kutta method [12, 13] Adam's or Gear's method [14, 15], the Bulirsch–Stoer extrapolation method [16], and others can be applied to obtain the solution. The selection of a particular method, however, depends on its computational efficiency, numerical accuracy and stability, and the 'stiffness' of the nonlinear system of differential equations. In this study, several numerical schemes are tested and finally the fifth- and sixth-order Runge–Kutta integrators, which are summarized in the Appendix, are determined to be satisfactory and are used for structural analysis in this paper.

7.1. *Single-degree-of-freedom systems*

Consider a one-story ($n = 1$) shear building with mass $m_1 = 1$, damping coefficient $c_1 = 0$ which consists of four different columns with the stiffnesses $k_{11} = 100$, $k_{12} = 200$, $k_{13} = 300$, $k_{14} = 400$, and the strengths $F_{11} = 960$, $F_{12} = 2400$, $F_{13} = 4800$, $F_{14} = 9600$. From the above physical properties with the parameter identification procedures proposed in [11], the time-invariant parameters of the local model are: $\mu_1 = 1$, $\beta_{11} = \gamma_{11} = 0.05$, $\beta_{12} = \gamma_{12} = 0.04$, $\beta_{13} = \gamma_{13} = 0.03$, $\beta_{14} = \gamma_{14} = 0.02$, and $A_{1l}(0) = 1$, $\alpha_{1l} = 0.04$, for all $l = 1, 2, 3, 4$. Note that the stiffness and strength characteristics are assumed to be widely different among the columns. Both nondegrading ($\delta_{A_{1l}} = 0$) and degrading ($\delta_{A_{1l}} \neq 0$) systems are considered. The above structural and material properties provide a complete local characterization of the

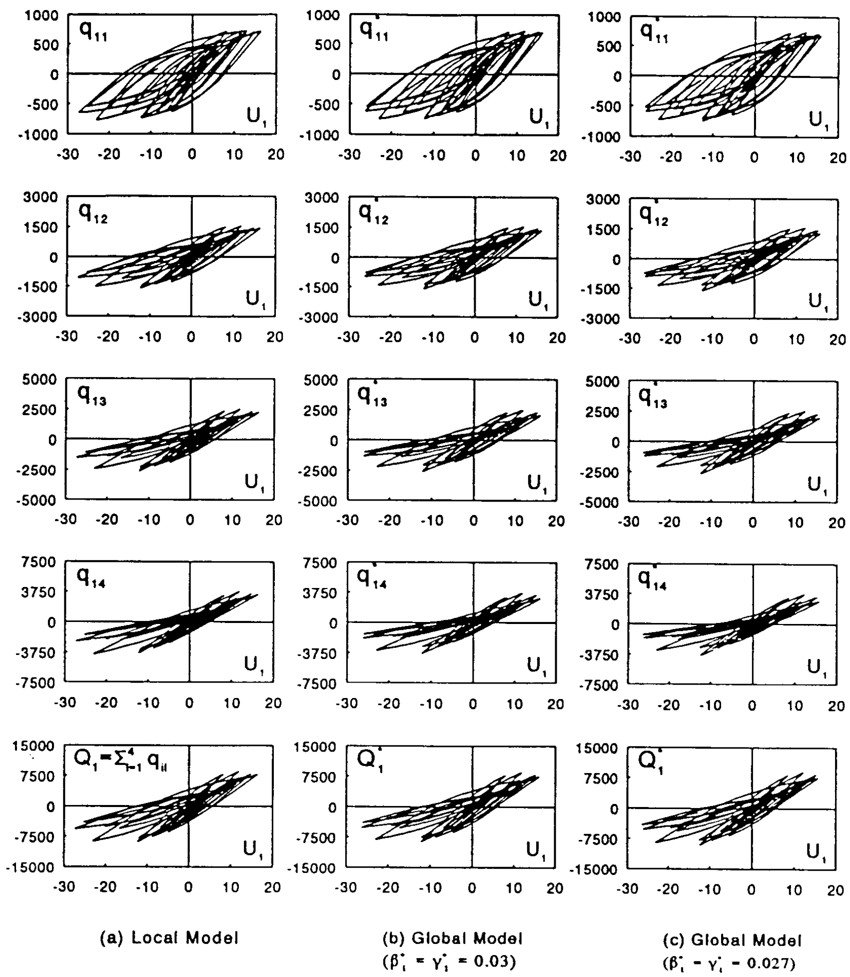

Fig. 8. Hysteretic loops for degrading system with $G_0 = 1.0 \times 10^5$.

nondegrading system. When the degrading system is considered, it is assumed to follow the deterioration rule in eqn (5), and the values of the additional parameters $\delta_{A_{1i}}$ for all the columns are taken as 5.0×10^{-6} in this study.

Suppose the nonlinear behavior of the building system can be approximated by a single hysteretic variable describing the restoring force for the building system itself. The time-invariant parameters corresponding to this global model can be calculated from eqns (17) and (19) as $k_1^* = 1000$, $A_1^*(0) = 1$, $\alpha_1^* = 0.04$, and $\mu_1^* = 1$, respectively. Two different estimates of β_1^* and γ_1^* are obtained following eqns (21) and (24). They are found to be $\beta_1^* = \gamma_1^* = 0.03$ and $\beta_1^* = \gamma_1^* = 0.027$, respectively. Obviously when the system is nondegrading ($\delta_{A_{1i}} = 0$), the global parameter $\delta_{A_1}^* = 0$ [eqn (27) or (28)]. For degrading system, the global rate of degradation $\delta_{A_1}^*$ is computed to be 1.5×10^{-6} by using eqn (28) or (29).

A sample of modulated Gaussian white noise of duration 6 s with a one-sided power spectral intensity G_0 scaled to unity is shown in Fig. 2. This simulated time-series multiplied by varying levels of intensity $G_0 = 1.0 \times 10^5$ and 1.0×10^7 are used as deterministic inputs to the single-degree-of-freedom nonlinear oscillator.

7.1.1. *Nondegrading system.* Figure 3(a) shows the time evolution of the relative displacement and velocity of the oscillator due to the deterministic forcing function in Fig. 2 with $G_0 = 1.0 \times 10^5$. The results of both local and global hysteretic models with two different estimates of β_1^* and γ_1^* are shown in the figure. Excellent agreement between these models is obtained irrespective of the approximations in eqns (21) and (24). No meaningful difference in response is noted due to the closeness of the bounds of the estimated global parameters. Also shown in Fig. 3(b) are the exact time variations of β_1^* and γ_1^* in eqn (20) in which the local hysteretic variables $Z_{1l}(t)$ are obtained following an analysis based on the local model. It clearly indicates the accuracy of the estimated global parameters β_1^* and γ_1^* from the proposed equations. The evolution of $Z_{1l}(t)$ mentioned above is shown in Fig. 3(c) which confirms the previous anticipation of a negligible time interval during which $Z_{1l}(t)$ are different. Accordingly, eqn (21) provides a simpler but useful approximation for global parameters. Figure 3(c) also shows the evolution of the displacement dependent story restoring forces

$$Q_1(t) = \sum_{l=1}^{4} q_{1l}(t)$$

with

$$q_{1l}(t) = \alpha_{1l} k_{1l} U_1(t) + (1 - \alpha_{1l}) k_{1l} Z_{1l}(t)$$

and

$$Q_1^*(t) = \alpha_1^* k_1^* U_1(t) + (1 - \alpha_1^*) k_1^* Z_1^*(t),$$

which are obtained from the local and global models, respectively. Again, very good agreement between the results of both models is obtained.

Figure 4(a) exhibits the plots of restoring forces $q_{1l}(t)$ and $Q_1(t)$ versus displacement $U_1(t)$ which are obtained from the local model thus providing hysteretic loops for individual columns and system itself. For comparison with the results of the global model, Figs 4(b) and 4(c) show similar kinds of plots of restoring force $Q_1^*(t)$ and the recovered column restoring forces $q_{1l}^*(t) = \alpha_{1l} k_{1l} U_1(t) + (1 - \alpha_{1l}) k_{1l} Z_{1l}^*(t)$ in which the conventional state variables $U_1(t)$ and $\dot{U}_1(t)$ are calculated from the global model [eqn (12)] and the recovered local hysteretic variables $Z_{1l}^*(t)$ are obtained by directly integrating eqn (4). They all indicate that the global model with both estimates of parameters β_1^* and γ_1^* can accurately predict both the local and global hysteretic characteristics of structural systems.

Figures 5 and 6 show similar sets of plots of various responses for a seismic input in Fig. 2 with a larger intensity of $G_0 = 1.0 \times 10^7$. The results of the global model with both estimates of parameters β_1^* and γ_1^* are found to be quite satisfactory when compared with those obtained from the local model. However, when the intensity is very large ($G_0 = 1.0 \times 10^7$), the response characteristics due to global models with estimated parameters $\beta_1^* = \gamma_1^* = 0.027$ are found to be superior to those obtained with $\beta_1^* = \gamma_1^* = 0.03$. This is due to the fact that for a significant amount of time the values of $Z_{1l}(t)$ as obtained from the local model and exhibited in Fig. 5(c) are equal to $Z_{1l,\max}(0) = [A_{1l}(0)/(\beta_{1l} + \gamma_{1l})]^{1/\mu_1}$. Due to the close proximity of the bounds, however, the results based on $\beta_1^* = \gamma_1^* = 0.03$ are still found to be reasonably good.

7.1.2. *Degrading system.* Figure 7(a) exhibits the time evolution of the displacement and velocity responses of the degrading oscillator for the

Table 1. Column properties and hysteretic parameters of local model for a five-story building frame

Story (k)	Column (l)	Stiffness k_{kl} (kN/mm)	Strength (kN)	$A_{kl}(0)$	β_{kl}	γ_{kl}	μ_k	$\delta_{A_{kl}}$	α_{kl}
1	1	19.22	91.23	1	0.064	−0.021	2	3.00E − 5	0.02
	2	46.89	272.53	1	0.043	−0.014	2	3.00E − 5	0.02
	3	46.89	272.53	1	0.043	−0.014	2	3.00E − 5	0.02
	4	19.22	91.23	1	0.064	−0.021	2	3.00E − 5	0.02
2	1	19.22	114.45	1	0.041	−0.014	2	3.36E − 5	0.02
	2	30.78	224.36	1	0.027	−0.009	2	3.36E − 5	0.02
	3	30.78	224.36	1	0.027	−0.009	2	3.36E − 5	0.02
	4	19.22	114.45	1	0.041	−0.014	2	3.36E − 5	0.02
3	1	19.22	129.44	1	0.032	−0.011	2	3.54E − 5	0.02
	2	19.22	161.82	1	0.021	−0.007	2	3.54E − 5	0.02
	3	19.22	161.82	1	0.021	−0.007	2	3.54E − 5	0.02
	4	19.22	129.44	1	0.032	−0.011	2	3.54E − 5	0.02
4	1	11.34	68.63	1	0.039	−0.013	2	3.36E − 5	0.02
	2	19.22	142.42	1	0.026	−0.009	2	3.36E − 5	0.02
	3	19.22	142.42	1	0.026	−0.009	2	3.36E − 5	0.02
	4	11.34	68.63	1	0.039	−0.013	2	3.36E − 5	0.02
5	1	11.34	48.17	1	0.080	−0.027	2	3.54E − 5	0.02
	2	11.34	58.94	1	0.053	−0.018	2	3.54E − 5	0.02
	3	11.34	58.94	1	0.053	−0.018	2	3.54E − 5	0.02
	4	11.34	48.17	1	0.080	−0.027	2	3.54E − 5	0.02

Table 2. Hysteretic parameters of global model for a five-story building frame

Story (k)	k_k^* (kN/mm)	β_k^*	γ_k^*	μ_k^*	A_k^*	δ_{Ak}^*	α_k^*
1	132.22	0.049	−0.016	2	1	8.85E − 6	0.02
2	100.00	0.032	−0.011	2	1	8.85E − 6	0.02
3	76.88	0.026	−0.009	2	1	8.85E − 6	0.02
4	61.12	0.031	−0.010	2	1	8.85E − 6	0.02
5	45.36	0.067	−0.022	2	1	8.85E − 6	0.02

deterministic input in Fig. 2 with intensity $G_0 = 1.0 \times 10^5$. The results are compared again with those obtained from the global models with two different estimates of β_1^* and γ_1^* as discussed earlier. As noted in the nondegrading systems, excellent agreement between the results of the local and global models are also obtained here for degrading systems. The exact time evolution of β_1^*, γ_1^* and $\delta_{A_1}^*$ in eqns (20) and (27) and the hysteretic variables $Z_{1l}(t)$ obtained from the local model are also shown, in Figs 7(b) and 7(c), respectively.

Figure 7(c) also shows the time evolution of restoring forces $Q_1(t)$ and $Q_1^*(t)$ obtained from the local and global hysteretic models. These story level restoring forces along with the column restoring forces $q_{1l}(t)$ and $q_{1l}^*(t)$ are also plotted against the

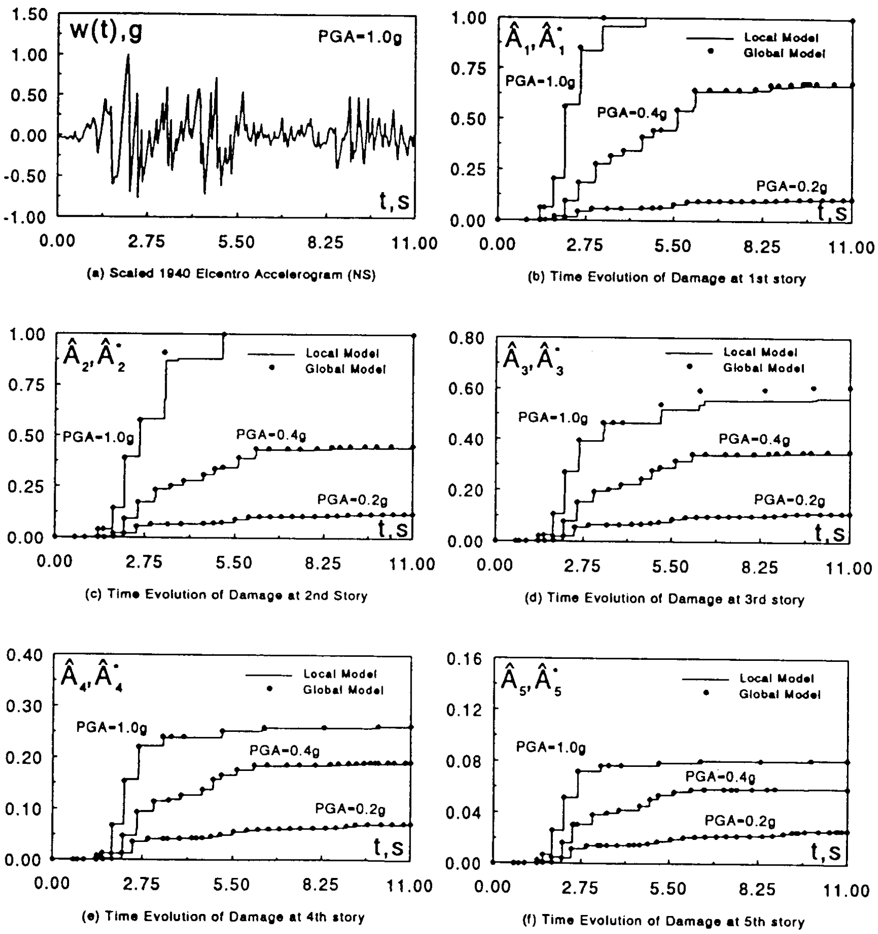

Fig. 9. Damage indices from seismic analysis of a five-story building frame.

displacement $U_1(t)$ in Fig. 8 providing various hysteretic loops. The results suggest that the global model with appropriate parameters can predict the hysteretic structural response of degrading systems with very good accuracy.

7.2. *Multi-degree-of-freedom systems*

Consider a five-story building frame designed according to the Uniform Building Code [17] for seismic zone-4. The building has four columns ($n_k = 4$) at each story and is idealized as a five-degree-of-freedom shear beam system with one degree of freedom per story. The lumped masses are $m_1 = m_2 = m_3 = m_4 = 0.0898$ kN sec^2 mm^{-1} for the first (bottom) to fourth stories and $m_5 = 0.0762$ kN sec^2 mm^{-1} for the fifth (top) story. The viscous damping coefficients are $c_1 = 0.844$ kN sec mm^{-1}, $c_2 = 0.638$ kN sec mm^{-1}, $c_3 = 0.491$ kN sec mm^{-1}, $c_4 = 0.390$ kN sec mm^{-1} and $c_5 = 0.288$ kN sec mm^{-1} for the bottom to top stories. The damping is assumed to be proportional to the initial stiffness matrix and the values of the above damping coefficients correspond to 3% of critical for the first mode. Table 1 provides the lateral stiffness and strength properties of the columns at each story and the parameters for the local hysteretic model.

Suppose the nonlinear behavior of this frame can be approximated by a single hysteretic variable for each story describing the global restoring force at that story. From the parameters of the local model in Table 1, the global parameters can be estimated based on eqns (17), (19), (21) and (28) proposed earlier. Table 2 provides these estimated values of these global parameters for each story.

In order to evaluate the global model, this five-story building frame is subjected to earthquakes to determine the structural damage predicted by both local and global models. A classical seismogram of the 1940 El Centro (NS component) earthquake with varying peak ground accelerations (PGA) is used as a deterministic input to this system. The above ground acceleration with scaled PGA equal to $1.0\,g$ ($1.0\,g = 9.81$ m/sec^2) is shown in Fig. 9(a).

A major objective of seismic design is the generation of structures that can survive earthquakes with a limited amount of damage. It has been proposed to evaluate structural performance by damage indices defined as scalar functions whose values can be related to particular structural (physical) damage states. In this paper, simple damage indices are defined based on the state of degrading parameters of hysteretic models (local and global). For example, consider the normalized damage indices $\hat{A}_k^*(t)$ and $\hat{A}_k(t)$ defined as

$$\hat{A}_k^*(t) = 1 - \frac{A_k^*(t)}{A_k^*(0)} \quad \text{and} \quad \hat{A}_k(t) = 1 - \frac{\sum_{l=1}^{4} w_{kl} A_{kl}(t)}{\sum_{l=1}^{4} w_{kl} A_{kl}(0)} \tag{30}$$

in which $A_k^*(t)$ and $A_{kl}(t)$ are the time-variant degrading parameters of the local and global restoring forces. In both cases, $\hat{A}_k^*(t)$ and $\hat{A}_k(t)$ represent the damage indices at the kth story obtained from the local and global models, respectively. Note that these indices are not calibrated to field data on the observed damage of actual building frames. However, from the values of $\hat{A}_k^*(t)$ and $\hat{A}_k(t)$, the corresponding stiffness and strength degradation can be evaluated.

Figures 9(b)–(f) show the time evolution of the damage indices $\hat{A}_k^*(t)$ and $\hat{A}_k(t)$ at the kth story ($k = 1, 2, \ldots, 5$) which is obtained for the deterministic seismic ground acceleration in Fig. 9(a) with various PGA $= 0.2\,g$, $0.4\,g$ and $1.0\,g$. Comparisons of results associated with local and global constitutive law suggest that the global hysteretic model with its parameters estimated from the proposed equations can predict structural damage with very good accuracy.

8. CONCLUSIONS

A global hysteretic model is developed and the relationship between the parameters of the local and global models is established for the seismic analysis of multi-story shear buildings. In both models, the analysis involves hysteretic constitutive laws commonly used in earthquake engineering to represent restoring forces and nonlinear dynamic analysis for estimating seismic structural response. From the proposed relationship, the local hysteretic behavior and damage can be obtained from an analysis based on global model. Using current global indices based on a heuristic combination of local damage measures, this was not possible due to the lack of a unique relationship between the lcoal and global damages.

Both nondegrading and degrading systems are considered and several numerical examples on single- and multi-degree-of-freedom systems of shear beam models are presented to illustrate the proposed methodology. First, a single-degree-of-freedom system with both nondegrading and degrading restoring forces is investigated to evaluate the adequacy of the global hysteretic model in predicting various seismic response characteristics. Second, a multi-degree-of-freedom system with a more realistic design and earthquake loading is studied to compare the damage measures by both the local and global hysteretic models. The results suggest that:

- the global model provides satisfactory estimates of traditional seismic response variables, such as displacement and velocity, when compared with those obtained from the analysis based on local model;
- the plots of restoring forces versus displacement, which represent the hysteretic loops, are well-predicted by the global model. When the local

hysteretic characteristics are recovered from dynamic analysis based on the global model, they are found to be in excellent agreement with the results produced by the local model; and
- using the proposed relationship between local and global parameters, the damage indices for a five-story shear frame predicted by the global hysteretic model compare very well with those obtained by the local hysteretic model.

In both local and global models, the dynamic stress analysis can be viewed as a nonlinear initial-value problem. However, the dimension of the global initial-value problem is much smaller than that of the local initial-value problem. Hence, significant savings of computational resources such as central processing units and core memory can be achieved by using the global model.

REFERENCES

1. Y. S. Chung, C. Meyer and M. Shinozuka, Seismic damage assessment of reinforced concrete members. Technical Report NCEER-87-0022, National Center for Earthquake Engineering Research, Buffalo, New York (1987).
2. Y. J. Park, A. M. Reinhorn and S. K. Kunnath, IDARC: Inelastic damage analysis of reinforced concrete frame–shear wall structures. Technical report, NCEER-87-0008, State University of New York at Buffalo, Buffalo, New York (1987).
3. S. Rahman, A Markov model for local and global damage indices in seismic analysis. Ph.D. dissertation presented to the Graduate School, Cornell University, Ithaca, New York (1991).
4. S. Rahman and M. Grigoriu, Markov model for seismic reliability analysis of degrading structures. *J. struct. Engng, ASCE* **119,** 1844–1865 (1993).
5. K. C. Valanis, A theory of viscoplasticity without a yield surface. *Archiwum Mechaniki Stossowanig* **23,** 517–551 (1971).
6. R. Bouc, Forced vibration of mechanical systems with hysteresis. *Proc. 4th Conf. Nonlinear Oscillation*, Prague, Czechoslovakia (1967).
7. Y. K. Wen, Method for random vibration of hysteretic systems. *J. Engng Mech. ASCE* **102,** 249–263 (1976).
8. Y. K. Wen, Equivalent linearization for hysteretic systems under random excitations. *J. appl. Mech., Trans. ASME* **47,** 150–154 (1980).
9. F. Casciati, Smoothed plasticity laws and elasto-plastic analysis. *Note Scientifiche in occasione del 70 deg Compleano*. Pubblicazione n. 179, Dell Universita di Pavia (1988).
10. T. T. Baber and Y. K. Wen, Stochastic equivalent linearization for hysteretic degrading multistorey structures. *Structural Research Series No. 471*, Department of Civil Engineering, University of Illinois at Urbana-Champaign, Urbana, IL (1980).
11. R. H. Sues, S. T. Mau and Y.-K. Wen, System identification of degrading hysteretic restoring forces. *J. Engng Mech., ASCE* **114,** 833–846 (1988).
12. C. Runge, Über die numerische Auflösung von Differentialgleichungen. *Math. Ann.* **46,** 167–178 (1895).
13. W. Kutta, Beitraz zur näherungsweisen Integration totaler Differentialgleichungen. *Z. Math. Phys.* **46,** 435–453 (1901).
14. C. W. Gear, *Numerical Initial Value Problems in Ordinary Differential Equations*. Prentice-Hall, Englewood Cliffs, NJ (1971).
15. L. F. Shampine and C. W. Gear, A user's view of solving stiff ordinary differential equations. *SIAM Rev.* **21,** 1–17 (1979).
16. R. Bulirsch and J. Stoer, Numerical treatment of ordinary differential equations by extrapolation methods. *Numerische mathematik* **8,** 1–13 (1966).
17. International Conference of Building Officials, *Uniform Building Code*. Whittier, CA (1988).
18. J. D. Lambert, *Computational Methods in Ordinary Differential Equations*. John Wiley, London (1973).
19. A. Huťa, Contribution à la formule de sixième ordre dans la méthode de Runge–Kutta–Nyström *Acta Fac. Rerum Natur. Univ. Comenian. Math.* **2,** 21–24 (1957).

APPENDIX: FIFTH- AND SIXTH-ORDER RUNGE–KUTTA METHOD

Consider the initial-value problem

$$\dot{\theta}(t) = h(\theta(t), t), \quad \theta(0) = \theta_0, \tag{A1}$$

where $t \in \mathscr{R}$ and $\theta \in \mathscr{R}$ are independent and dependent variables, respectively. A general explicit one-step method for the solution of eqn (A1) is given by [12, 13]

$$\theta_{t+1} - \theta_t = \Delta t \varphi(t_t, \theta_t; \Delta t), \tag{A2}$$

where t_t is a discrete value of independent variable $t, \theta_t = \theta(t_t)$, and $\varphi(\cdot)$ will be defined later. The general R-stage explicit Runge–Kutta method is defined by eqn (A2) in which

$$\varphi(t, \theta; \Delta t) = \sum_{r=1}^{R} A_r K_r, \tag{A3}$$

where

$$K_1 = h(t, \theta)$$

$$K_r = h\left(t + \Delta t \sum_{s=1}^{r-1} B_{rs}, \theta + \Delta t \sum_{s=1}^{r-1} B_{rs} K_s\right), \quad r = 2, 3, \ldots, R \tag{A4}$$

with A_r and B_{rs} as appropriate constants. Note that an R-stage Runge–Kutta method involves R function evaluations per step. Each of the functions $K_r(t, \theta; \Delta t)$, $r = 1, 2, \ldots, R$, may be interpreted as an approximation to the time derivative $\dot{\theta}$, and the functions $\varphi(t, \theta(t); \Delta t)$ as the weighted average of these approximations. For examples, the six-stage fifth-order method is [18]

$$\theta_{t+1} - \theta_t = \frac{\Delta t}{192}(23K_1 + 125K_3 - 81K_5 + 125K_6), \tag{A5}$$

where

$$K_1 = h(t_t, \theta_t)$$

$$K_2 = h(t_t + \tfrac{1}{3}\Delta t, \theta_t + \tfrac{1}{3}\Delta t K_1)$$

$$K_3 = h(t_t + \tfrac{2}{5}\Delta t, \theta_t + \tfrac{1}{25}\Delta t[4K_1 + 6K_2])$$

$$K_4 = h(t_i + \Delta t, \theta_i + \tfrac{1}{4}\Delta t[K_1 - 12K_2 + 15K_3])$$

$$K_5 = h(t_i + \tfrac{2}{3}\Delta t, \theta_i + \tfrac{1}{81}\Delta t[6K_1 + 90K_2 - 50K_3 + 8K_4])$$

$$K_6 = h(t_i + \tfrac{4}{5}\Delta t, \theta_i + \tfrac{1}{75}\Delta t[6K_1 + 36K_2 + 10K_3 + 8K_4]) \qquad \text{(A6)}$$

and the eight-stage sixth order method is [19]

$$\theta_{i+1} - \theta_i = \frac{\Delta t}{840}(41K_1 + 216K_3 + 27K_4 + 272K_5 + 27K_6 + 216K_7 + 41K_8), \qquad \text{(A7)}$$

where

$$K_1 = h(t_i, \theta_i)$$

$$K_2 = h(t_i + \tfrac{1}{9}\Delta t, \theta_i + \tfrac{1}{9}\Delta t K_1)$$

$$K_3 = h(t_i + \tfrac{1}{6}\Delta t, \theta_i + \tfrac{1}{24}\Delta t[K_1 + 3K_2])$$

$$K_4 = h(t_i + \tfrac{1}{3}\Delta t, \theta_i + \tfrac{1}{6}\Delta t[K_1 - 3K_2 + 4K_3])$$

$$K_5 = h(t_i + \tfrac{1}{2}\Delta t, \theta_i + \tfrac{1}{8}\Delta t[-5K_1 + 27K_2 - 24K_3 + 6K_4])$$

$$K_6 = h(t_i + \tfrac{2}{3}\Delta t, \theta_i + \tfrac{1}{9}\Delta t[221K_1 - 981K_2 + 867K_3 - 102K_4 + K_5])$$

$$K_7 = h(t_i + \tfrac{5}{6}\Delta t, \theta_i + \tfrac{1}{48}\Delta t[-183K_1 + 678K_2 - 472K_3 - 66K_4 + 80K_5 + 3K_6])$$

$$K_8 = h(t_i + \Delta t, \theta_i + \tfrac{1}{82}\Delta t[716K_1 - 2079K_2 + 1002K_3 + 834K_4 - 454K_5 - 9K_6 + 72K_7]). \qquad \text{(A8)}$$